

In-plane vortex-lattice depinning in a layered superconductor

M. F. Crommie, G. Briceño, and A. Zettl

*Department of Physics, University of California at Berkeley, Berkeley, California 94720
and Materials Sciences Division of the Lawrence Berkeley Laboratory, Berkeley, California 94720*

(Received 13 March 1992)

The out-of-plane (c -axis) dissipation of the layered superconductor $\text{Bi}_2\text{Sr}_2\text{CaCu}_2\text{O}_8$ has been probed in the mixed state by current-voltage (I - V) measurements. Distinctly different behavior is observed for magnetic field \mathbf{H} oriented parallel (\parallel) and perpendicular (\perp) to c , suggestive of two different out-of-plane dissipation mechanisms. We interpret our results for $\mathbf{H}\perp c$ as arising from Josephson vortex dynamics.

One of the most intensively studied aspects of the high- T_c oxides is their response to a transport current in the mixed state. Attempts have been made to explain the dissipation observed in the mixed state through various models, some involving Abrikosov vortex motion¹ and some not.^{2,3} Despite the volume of work performed, however, there is still much controversy over the nature of this dissipation, as well as over the magnitudes of such fundamental parameters as the anisotropic coherence length and penetration depth.⁴⁻⁶ One source of confusion is the uncertainty of whether data should be interpreted in terms of the three-dimensional effective mass Ginzburg-Landau equations, or the differential-difference equations more appropriate in the quasi-two-dimensional regime of weakly coupled superconducting layers.⁷ This problem is especially central to the more anisotropic superconductors such as $\text{Bi}_2\text{Sr}_2\text{CaCu}_2\text{O}_8$.

To address these issues, we have measured the c -axis current-voltage (I - V) characteristics of single-crystal $\text{Bi}_2\text{Sr}_2\text{CaCu}_2\text{O}_8$ in a strong magnetic field, \mathbf{H} , both parallel and perpendicular to the c axis. The voltage along c was measured while passing current through the crystal in the c direction. We observe no c -axis critical current for $\mathbf{H}\parallel c$, while for $\mathbf{H}\perp c$ (\mathbf{H} along the CuO layers) a temperature and magnetic-field-dependent c -axis critical current is obtained. The behavior observed when $\mathbf{H}\perp c$ is shown to be intrinsically distinct from the case where $\mathbf{H}\parallel c$, as opposed to being the result of an "error" component of \mathbf{H} along c (H_{\parallel}). For $\mathbf{H}\perp c$, we interpret the observed critical current as signalling the depinning of a Josephson vortex lattice. This phenomenon is likened to the behavior of fluxons pinned by random inhomogeneities in a long Josephson junction.

Single-crystal samples of $\text{Bi}_2\text{Sr}_2\text{CaCu}_2\text{O}_8$ having average dimensions of $1\times 1\times 0.010$ mm³ used in this study.³ Low resistance contacts (~ 1 Ω) were made to the samples using fired on silver pads. The contact geometry employed was a four-point concentric ring configuration,³ used to create as uniform a current density (\mathbf{J}) as possible for \mathbf{J} parallel to c . The dc I - V 's were taken by incrementally ramping the current through the sample with a dc current source, while measuring dc voltage (with a sensitivity better than 2×10^{-8} V) at each point with a Keithly 181 nanovoltmeter. Specially constructed electronic filters shielded both the sample's current and voltage leads

from any possible high-frequency noise originating in external circuitry. Pulsed I - V 's were also performed to confirm that sample joule heating was not significant. As a further check on the experimental setup, dc I - V 's were taken of a known linear resistor whose resistance was comparable to that of the mixed-state $\text{Bi}_2\text{Sr}_2\text{CaCu}_2\text{O}_8$ crystals.

Figure 1(a) shows the c -axis I - V characteristics of single-crystal $\text{Bi}_2\text{Sr}_2\text{CaCu}_2\text{O}_8$ for $H=7.5$ T $\parallel c$, measured between $T=25$ and 55 K. The I - V 's are linear at low current density and high temperature, but show signs of nonlinearity in the high current region at lower temperatures. The extent of the linear region is sample dependent, but the overall behavior is qualitatively similar from sample to sample. At this high field the I - V 's are all linear for $T>55$ K. No sign of a critical current is observed in the $\mathbf{H}\parallel c$ configuration, as reflected in the fact that the curvature of the log-log plot is always positive or zero. Figure 1(b) shows a linear plot of the low current region of the same I - V 's shown in Fig. 1(a). Each curve is normalized by E ($J\sim 3000$ A/m²) and vertically offset, thus emphasizing the temperature dependence of the shape of the I - V 's.

The c -axis dissipation is remarkably different when $\mathbf{H}\perp c$. Figure 2(a) shows the I - V characteristics for the same sample shown in Fig. 1, with $H=7.5$ T $\perp c$. While the I - V 's all become linear at high currents and high temperature, the I - V 's for $T\leq 73$ K show negative curvature in the log-log plot. From the expanded linear plots of the I - V 's in Fig. 2(b), this negative curvature is seen to arise from the existence of a nonzero critical current, J_c , for temperatures up to $T\sim 73$ K. We note that, for lower values of H , nonzero critical currents were seen at even higher temperatures. The I - V 's shown in Fig. 2(b) have each been normalized by E ($J=170$ A/m²), and vertically offset.

Figure 3 shows the detailed temperature and field dependence of J_c ($\mathbf{H}\perp c$). The temperature dependence of J_c at $H=7.5$ T is shown for the same crystal described in Figs. 1 and 2. J_c is determined by fitting a straight line to the finite voltage data and picking off the x -axis (current) intercept. The inset in Fig. 3 shows the magnetic-field dependence of J_c at $T=55$ K for a different sample. J_c falls monotonically to zero with increasing temperature and magnetic field.

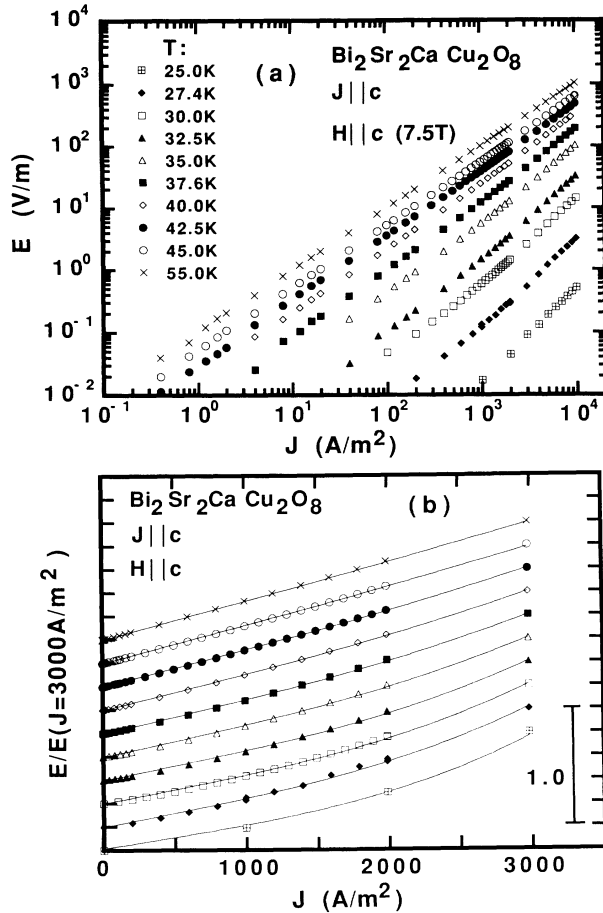


FIG. 1. *c*-axis *I-V* characteristics for $H=7.5$ T applied parallel to *c*. (a) log-log axes. (b) Low current region, linear axes; solid lines are guides to the eye. The same symbols represent the same temperatures in (a) and (b).

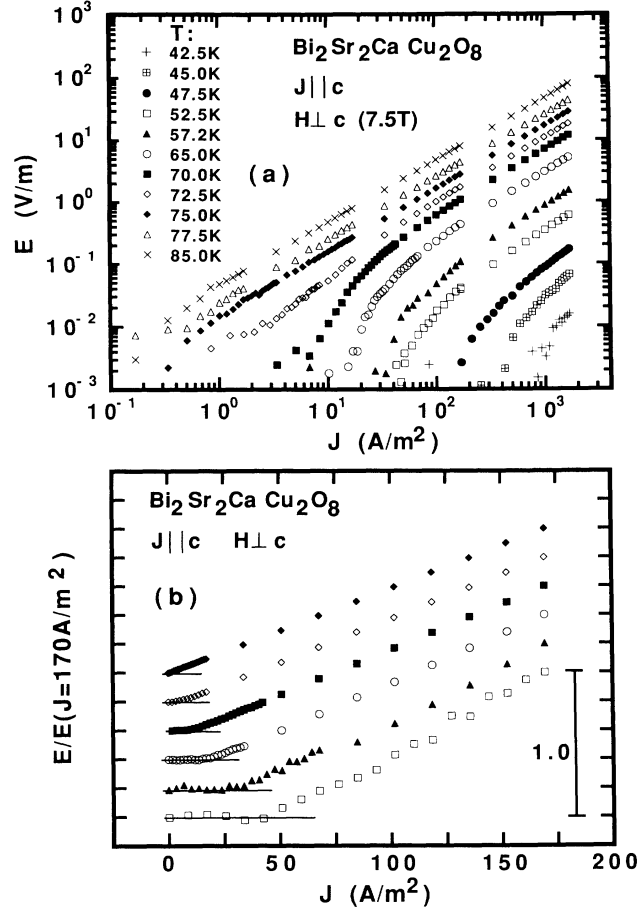


FIG. 2. *c* axis *I-V* characteristics for $H=7.5$ T applied perpendicular to *c*. (a) log-log axes. (b) Low current region, linear axes; solid lines represent zero voltage. The same symbols represent the same temperatures in (a) and (b).

As seen from Figs. 1 and 2, the *c*-axis *I-V*'s show very different behavior depending on whether \mathbf{H} is parallel or perpendicular to *c*. It is difficult, even in principle, to reconcile the *I-V*'s for $\mathbf{H}\perp c$ and $\mathbf{H}\parallel c$ with a common mechanism involving the motion of three-dimensional Abrikosov vortices. To see this one must first recognize that the generation of an electric field parallel to *c* (inter-layer voltage) requires in-plane motion of a vortex segment parallel to the CuO planes (since $\mathbf{E}\sim\mathbf{v}\times\mathbf{B}$). One would expect that, for in-plane motion, the pinning of Abrikosov vortices would be greater when $\mathbf{H}\parallel c$ (i.e., when vortices pierce the CuO planes) than when $\mathbf{H}\perp c$. The reason for this is that the energy gained by core pinning to a defect in a superconducting layer is greater than that gained by pinning to a defect between layers (where the order parameter is depressed).⁸ In addition, for $\mathbf{J}\parallel c$ the Lorentz force density on Abrikosov vortices with $\mathbf{H}\perp c$ would be greater than on vortices with $\mathbf{H}\parallel c$. These considerations lead to the conclusion that, for a given value of *H*, the *c*-axis critical current should be lower and the *c*-axis dissipation greater for $\mathbf{H}\perp c$ than for $\mathbf{H}\parallel c$. Experimentally, however, as seen from Figs. 1 and 2, exactly the opposite occurs.

From experiments showing Lorentz force indepen-

dence⁹ and peculiar scaling behavior in the *ab*-plane mixed-state resistivity of $\text{Bi}_2\text{Sr}_2\text{CaCu}_2\text{O}_8$ (as well as from magnetization results)¹⁰ it has been suggested that mixed-state dissipation in $\text{Bi}_2\text{Sr}_2\text{CaCu}_2\text{O}_8$ is due only to H_{\parallel} .¹⁰ If this were true for out-of-plane transport as well,

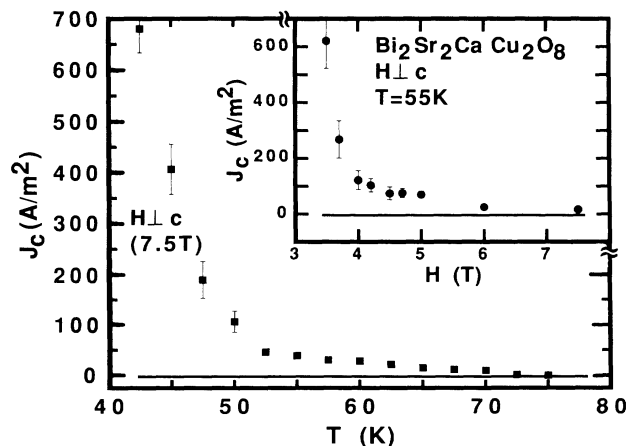


FIG. 3. Temperature dependence of J_c for $\mathbf{H}\perp c$. Inset: *H* dependence of J_c at $T=55$ K.

then it would imply that the behavior seen in Figs. 1 and 2 represents two different limits of the same basic phenomena, and that *all* of the c -axis I - V 's should scale with H_{\parallel} . The I - V 's for $H \perp c$ would then be wholly determined by H_{\parallel} . In order to check this hypothesis, a c -axis I - V was first taken at $T = 65$ K with $H = 7.5$ T $\perp c$. The crystal was then rotated to make $H \parallel c$, while the temperature remained constant. The magnetic field was subsequently ramped down to $H = 0.4$ T ($\parallel c$), at which point the I - V was measured to have the same slope at high current as the previous I - V with $H \perp c$. Assuming the scaling (i.e., error component) hypothesis to be correct for c -axis transport, then the two I - V 's should be identical. Experimentally, however, the two I - V 's are different, as shown in Fig. 4. The $H \parallel c$ I - V is completely linear in the low current regime while the $H \perp c$ I - V displays a sharp critical current. The nonexistence of an $H \parallel c$ "error" field, at which the value the $H \perp c$ behavior would be recovered, demonstrates unambiguously the distinct nature of the c -axis dissipation observed in these two magnetic-field orientations.

The question then remains as to the origin of the dissipation observed in these two experimental configurations. For $H \parallel c$ the situation is complicated by the lack of a macroscopic Lorentz force. In Ref. 3 it was argued that dissipation in this geometry is caused by temperature activated phase slip across weak links in the sample. In the limit of small current density, this model predicts a linear I - V . Linear I - V 's are, indeed, seen in Fig. 1 at high temperatures and low currents, but at the lowest temperatures and highest currents the I - V 's deviate from linearity. The origin of the nonlinearity is not obvious, but could possibly arise from critical current inhomogeneities or a competing effect such as helical instabilities.¹¹

We now concentrate on the case where $H \perp c$. Theodorakis¹² has recently shown theoretically that in a weakly Josephson-coupled layered superconductor there can be two coexisting the decoupled vortex lattices: an Abrikosov vortex lattice from the component of H parallel to c , and a Josephson vortex lattice from the component of H perpen-

dicular to c . The vortices in the Josephson vortex lattice fit between the layers, each vortex having a width of $\Phi_0/H_{\perp}d$, where d is the distance between layers and H_{\perp} is the component of H perpendicular to c . Unlike the Abrikosov vortices, the Josephson vortices are not associated with zeros in the order parameter (normal cores). Consideration of the dissipative effects of such Josephson vortices in high- T_c superconductors has been largely neglected, possibly because an in-plane Lorentz force can be exerted upon them only by passing a current parallel to the c axis (which is not the conventional current direction). We believe that the c -axis I - V 's shown here for $H \perp c$ give evidence of dissipation due to the depinning of a Josephson vortex lattice in $\text{Bi}_2\text{Sr}_2\text{CaCu}_2\text{O}_8$. Recent high- Q oscillator measurements¹³ also suggest a role played by Josephson vortices in the mechanical oscillator response of $\text{Bi}_2\text{Sr}_2\text{CaCu}_2\text{O}_8$ in an H field.

In the absence of a detailed theory of the motion of a Josephson vortex lattice in high- T_c oxides, we make an analogy to the more familiar case of a single Josephson tunnel junction threaded by H . Here the junction's behavior depends on whether the length of the junction, L , is greater or smaller than the Josephson penetration depth¹⁴ $\lambda_J = (c\Phi_0/8\pi^2J_c d')^{0.5}$, where J_c is the junction's zero-field critical current density and d' is its effective barrier thickness. If $\lambda_J \gg L$, then self-screening effects can be ignored, while in the opposite limit they must be considered. Following the suggestion of Ref. 12 that the vortices reside between each CuO layer ($d' \sim 15$ Å), and using the bulk $J_c \sim 10^6$ A/cm² (Ref. 3), we find $\lambda_J \sim 4$ μm. As $L \sim 1$ mm for our crystals, we are clearly in the limit where screening is important. In this "long junction" limit the behavior of the Josephson vortices is determined by the nonlinear partial differential equation¹⁴

$$\frac{\partial^2 \phi}{\partial x^2} - \frac{1}{c'^2} \frac{\partial^2 \phi}{\partial t^2} - \frac{\beta}{c'^2} \frac{\partial \phi}{\partial t} = \lambda_J^{-2} \sin \phi, \quad (1)$$

where $\phi(x, t)$ represents the time and position-dependent phase across the junction, while c' and β depend on the geometry and shunting of the junction.

The motion of a single Josephson vortex solution to Eq. (1) in the presence of pinning has been considered.^{15,16} Pinning is described as arising from spatial inhomogeneities in λ_J , i.e., from "micro-shorts" and "micro-resistances" across the junction. The behavior of the Josephson vortex in the presence of pinning is similar to what one would expect from an Abrikosov vortex in a type-II superconductor: The vortex stays pinned as the current is increased until the Lorentz force on the vortex overcomes the pinning force. In this scenario the temperature dependence of the critical current shown in Fig. 3 is accounted for by temperature-activated defects¹⁷ or "shorts" on or between the CuO planes of the $\text{Bi}_2\text{Sr}_2\text{CaCu}_2\text{O}_8$ crystal.

Unfortunately, we are unaware of any solutions to Eq. (1) in the presence of pinning *and* a strong magnetic field. At the high fields accessed in this study, however, the sample will be packed tightly with magnetic flux. As a result, collective interactions, as well as field-dependent inhomogeneities (such as any coexisting Abrikosov vortices arising from H_{\parallel} [Ref. 16]), must be considered to explain

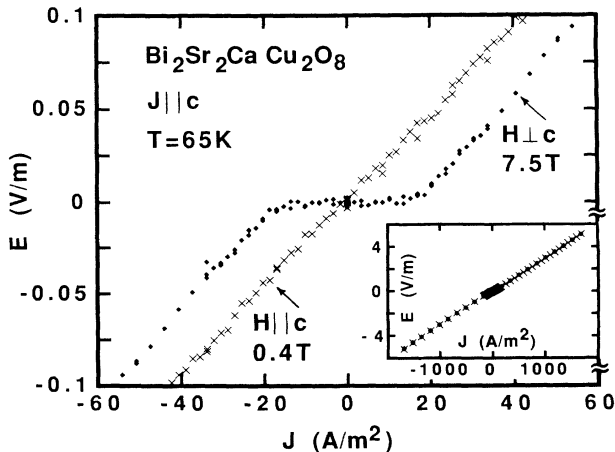


FIG. 4. I - V characteristics for $H \parallel c$ (0.4 T) and $H \perp c$ (7.5 T). The curves have identical slopes at high applied current (see inset), but dramatically different behavior near the origin.

the H -field dependence of the critical current shown in the inset of Fig. 3. In this limit one might expect a stiffening of the Josephson vortex lattice with increasing H .¹⁸ An increasing lattice stiffness would allow the vortices to "ride" over pins with less difficulty, resulting in a decreasing critical current with increasing H , as observed experimentally in Fig. 3 for $\text{Bi}_2\text{Sr}_2\text{CaCu}_2\text{O}_8$.

The existence of an independent, sliding Josephson vortex lattice for $\mathbf{H} \perp c$ in $\text{Bi}_2\text{Sr}_2\text{CaCu}_2\text{O}_8$ helps reconcile the results of other experiments with our own. Here we refer to the experimental results (ab -plane transport and magnetization) discussed in Ref. 10 where it is concluded that although an in-plane Josephson vortex lattice might exist, dissipation occurs only from the motion of coexisting Abrikosov vortices parallel to c . This conclusion is con-

sistent with our own results if the Josephson vortex lattice remains static under the influence of in-plane current. This is reasonable since an in-plane Lorentz force cannot be applied to such vortices by an in-plane current.

Note added. Recent magnetotransport experiments by Latyshev and Volkov¹⁹ give additional evidence for Josephson vortex dynamics in $\text{Bi}_2\text{Sr}_2\text{CaCu}_2\text{O}_8$.

We wish to acknowledge useful conversations with M. J. Ferrari, F. C. Wellstood, and D. S. Rokhsar. This work was supported by the Director, Office of Energy Research, Office of Basic Energy Sciences, Materials Sciences Division of the U.S. Department of Energy under Contract No. DE-AC03-76SF00098. M.F.C. acknowledges additional support from the Department of Education.

- ¹T. T. M. Palstra *et al.*, Phys. Rev. B **41**, 6621 (1990); R. B. van Dover *et al.*, *ibid.* **39**, 4800 (1989).
²D. H. Kim *et al.*, Phys. Rev. B **42**, 6249 (1990).
³G. Briceño, M. F. Crommie, and A. Zettl, Phys. Rev. Lett. **66**, 2164 (1991).
⁴A. P. Malozemoff *et al.*, Physica C **162-164**, 353 (1989).
⁵B. D. Biggs *et al.*, Phys. Rev. B **39**, 7309 (1989).
⁶M. Tuominen *et al.*, Phys. Rev. B **42**, 412 (1990).
⁷L. N. Bulaevskii *et al.*, Zh. Eksp. Teor. Fiz. **94**, 355 (1988) [Sov. Phys. JETP **67**, 1499 (1988)].
⁸D. Feinberg and C. Villard, Phys. Rev. Lett. **65**, 919 (1990).
⁹Y. Iye, S. Nakamura, and T. Tamegai, Physica C **159**, 433 (1989); Y. Iye, T. Tamegai, and S. Nakamura, *ibid.* **174**, 227 (1991).
¹⁰P. H. Kes *et al.*, Phys. Rev. Lett. **64**, 1063 (1990); see also H. Raffy *et al.*, *ibid.* **66**, 2515 (1991).

- ¹¹E. H. Brandt, Phys. Rev. B **25**, 5756 (1982).
¹²Stavros Theodorakis, Phys. Rev. B **42**, 10172 (1990).
¹³C. Duran *et al.*, Phys. Rev. B **44**, 7737 (1991).
¹⁴A. Barone and G. Paternó, *Physics and Applications of the Josephson Effect* (Wiley, New York, 1982), Chaps. 4 and 10 (note that Gaussian units are used here).
¹⁵M. B. Mineev, M. V. Feigel'man, and V. V. Schmidt, Zh. Eksp. Teor. Fiz. **81**, 290 (1981) [Sov. Phys. JETP **54**, 155 (1981)].
¹⁶Y. S. Kivshar and O. A. Chubykalo, Phys. Rev. B **43**, 5419 (1991).
¹⁷J. C. Phillips, *Physics of High- T_c Superconductors* (Academic, Boston, 1989), Chap. 4.
¹⁸K. Yoshida, F. Irie, and K. Hamasaki, J. Appl. Phys. **49**, 4468 (1978).
¹⁹Y. I. Latyshev and A. F. Volkov, Physica C **182**, 47 (1991).